Article

Not peer-reviewed version

Neutral and Ionic Form of (Benzylthio)acetic Acid in Novel Aminopyrimidine Based Multi-Component Crystalline Phases

Justyna Sienkiewicz-Gromiuk * and Aleksandra Drzewiecka-Antonik

Posted Date: 31 October 2023

doi: 10.20944/preprints202310.1982.v1

Keywords: (benzylthio)acetic acid; aminopyrimidines; supramolecular organic frameworks (SOFs); co-crystal; salt solvate; nonbonding contacts; SC XRD structural analysis; FT-IR spectroscopy; thermal study

Article

Neutral and Ionic Form of (Benzylthio)Acetic Acid in Novel Aminopyrimidine Based Multi-Component Crystalline Phases

Justyna Sienkiewicz-Gromiuk [1,*] and Aleksandra Drzewiecka-Antonik [2]

[1] Department of General and Coordination Chemistry and Crystallography, Institute of Chemical Sciences, Faculty of Chemistry, Maria Curie-Sklodowska University in Lublin, M. Curie-Sklodowska Sq. 2, 20-031 Lublin, Poland; justyna.sienkiewicz-gromiuk@mail.umcs.pl
[2] Institute of Physics, Polish Academy of Sciences, Aleja Lotnikow 32/46, 02-668 Warsaw, Poland; adrzew@ifpan.edu.pl
* Correspondence: justyna.sienkiewicz-gromiuk@mail.umcs.pl

Abstract: The (benzylthio)acetic acid (HBTA) and some aminopyrimidines, namely 2-aminopyrimidine (2-AP), 5-aminopyrimidine (5-AP), 2-amino-4,6-dimethylpyrimidine (2-A-4,6-DMP) and 2,4,6-triaminopyrimidine (2,4,6-TAP), were successfully embodied as structural units into the construction of a total of four novel supramolecular organic frameworks. The received crystalline solids were inspected by single crystal X-ray diffraction (SC XRD) in order to obtain insight into the structural and supramolecular facets. The SOFs deriving from 2-AP, 5-AP as well as 2-A-4,6-DMP crystallize in the form of true co-crystals (**1**-**3**), while the one originating from 2,4,6-TAP crystallizes as salt solvate (**4**). The SC XRD results indicated the different contents of structural residues present in the asymmetric units of the crystals **1**-**4** despite the using the same molar ratio of molecular co-formers in each case. The molecular structures of co-crystals **1**-**3** consist of either one neutral residue of each starting components (**1** and **3**) or a half nonionized residue of aminopyrimidine ingredient and one neutral residue of acidic specie (**2**). The asymmetric unit of salt solvate **4** is composed of two ionized residues of each co-former (two 2,4,6-TAP$^+$ cations and two BTA$^-$ anions) and one MeOH solvent molecule. The most extensive H-bonding network is observed in the crystal structure of salt solvate **4**. The relevant molecular ingredients in co-crystals **1**-**3** are mainly hold together by the neutral $O_{carboxylic}–H\cdots N_{pyrimidine}$ and $N_{amine}–H\cdots O_{carboxylic}$ H-bonds. In the case of aggregate **4**, the corresponding ionic residues are predominantly sustained by the charged-assisted $N_{pyrimidinium}–H\cdots O_{carboxylate}$ and $N_{amine}–H\cdots O_{carboxylate}$ hydrogen interactions. The MeOH solvent incorporated into the crystal lattice of adduct **4** is also involved in H-bonding by simultaneously serving as the single donor in $O_{MeOH}–H\cdots S$ and the single acceptor in $N_{amine}–H\cdots O_{MeOH}$ H-bonds afforded the structural diversity within the 2,4,6-TAP$^+$ cations and BTA$^-$ anions. Other weaker sets of additional non-covalent contacts existing in the crystal structures of analyzed conglomerates are involved in the self-assembly, stabilization and expansion of total supramolecular organic frameworks. The fact of the formation of non-covalent bonded supramolecular organic frameworks in question is also reflected in corresponding results obtained through elemental analysis (EA), Fourier transform infrared spectroscopy (FT−IR) and thermal analysis (TG/DSC).

Keywords: (benzylthio)acetic acid; aminopyrimidines; supramolecular organic frameworks (SOFs); co-crystal; salt solvate; nonbonding contacts; SC XRD structural analysis; FT-IR spectroscopy; thermal study

1. Introduction

The supramolecular organic frameworks (SOFs), also known the multi-component crystalline solids/phases or multi-component molecular crystals are the group of materials fabricated using the supramolecular crystal engineering [1]. The supramolecular conglomerates are formed as a result of

doi:10.20944/preprints202310.1982.v1

spontaneous intermolecular self-assembling achieved by creating various bunch of non-covalent interactions between the favorable functional groups that build up the molecules of organic co-partners [2]. The occurrence of the different non-covalent contacts, embracing the classical and nonclassical H-bonds, electrostatic forces, $\pi\cdots\pi$ stacking, π-cation and π-anion, lone pair-π attractions and the other ones, is necessary factor to direct the molecular arrangement in the crystals [3]. The process of intermolecular association based on the development of combination of classical H-bonds and complementary weak non-covalent forces is responsible for fabrication of the specific crystal structures bearing particular physicochemical properties [4].

The carboxylic acids and basic N-heterocyclic derivatives are very often employed in crystal engineering as effective building tectons in the production of new supramolecular organic frameworks (SOFs). Their leader position as building bricks in the process of engendering the multi-component organic crystalline phases is dictated by their chemical composition characterized by bearing an excellent donor and acceptor moieties susceptible to effective organic acidic-basic supramolecular complexation. The most important functional group of organic acids, that strongly interacts with other organic partners with basic nature, is –COOH group. The acidic-basic supramolecular aggregation is carried out by the facilitated formation of the neutral N–H···O/O–H···N or charged-assisted N^{+}–H···O^{-} and N–H···O^{-} H-bonds enclosed between pyrimidine/amine groups equipped with the lone electron pair localized on the nitrogen atoms of base ingredients and complementary caroboxylic/carboxylate groups derived from acidic co-formers. These neutral or charged-assisted strong H-bonds, holding the acidic and basic components together, influence the crystalline form of the resulting multi-component molecular materials in the co-crystal/salt category. An introduction of the extra potential binding spacers (CH, CH_2, CH_3, aryl core, halogens, OH, S, O, SO_2, NO_2) into the chemical structure of implemented co-partners yielded the more complicated networks of non-covalent forces that ultimately causes changes in the crystal packing as well as features of supramolecular solids [5–7].

A literature survey unveiled the aminopirymidine compounds have been filed to supramolecular complexation with large number of carboxylic acids. The selected aminopyrimidines in the form of 2-aminopyrimidine (2-AP), 5-aminoaminopyrimidine (5-AP), 2-amino-4,6-dimethylpyrimidine (2-A-4,6-DMP) and 2,4,6-triaminopyrimidine (2,4,6-TAP) (Figure 1) fit perfectly into generating the non-covalent bonding with various acidic derivatives due to the presence of three or five basic nitrogen sites.

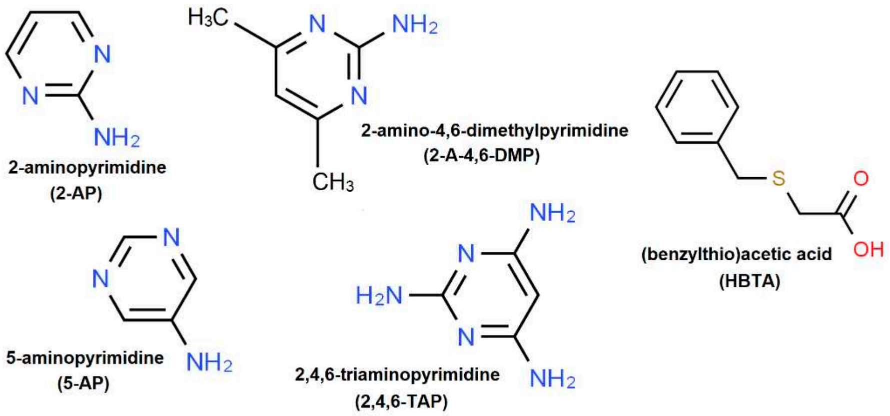

Figure 1. Chemical formula of selected H-bond building blocks.

The CSD analysis [8] based on the *ConQuest 2022.3.0* software [9] showed that the 2-AP and 2-A-4,6-DMP interact most readily with carboxylic co-partners giving the 64 and 58 multi-component molecular crystals, respectively (Figure 2A). The 2,4,6-TAP specie were enclosed only in the 19 supramolecular architectures, whereas no data regarding the utility of 5-AP as a building brick in the supramolecular complexation were found (Figure 2A). The 2-AP as well as 2-A-4,6-DMP remain in their neutral figure in the majority of disclosed crystal structures obtained with the participation of carboxylic co-formers, which constitute the 64.1 % and 67.2 % of total number of acid:base supramolecules, respectively. The structural results published in the CSD database [8,9] and gathered in Figure 2B indicate that solely the 2-A-4,6-DMP entity builds the supramolecular complexes within all specified subclasses of multi-component crystalline phases [10].

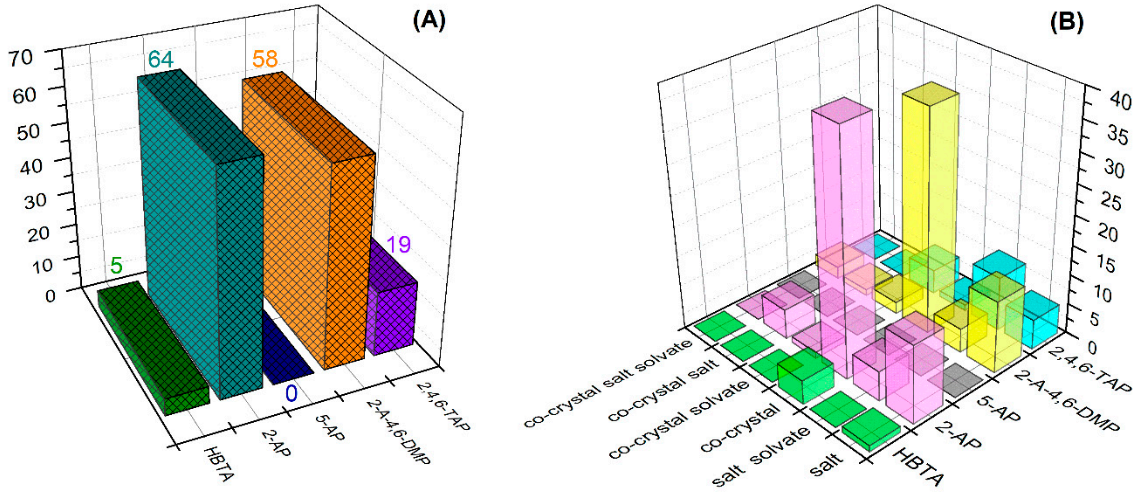

Figure 2. The number of reported crystal structures (A) along with the summary of crystalline forms (B) of multi-component molecular crystals containing HBTA:N-heterocycles as well as carboxylic acids:2-AP/2-A-4,6-DMP/2,4,6-TAP synthons, respectively.

The supramolecular conglomerates fabricated from 2-AP and carboxylic co-partners generate two- or three-component molecular crystals belonging to almost all defined subclasses of SOFs [10], except the salt co-crystal solvate (Figure 2B). The 2-AP generally forms supramolecular adducts without any solvent as evidenced by only six reported acid:base crystalline solids containing solvent residues in the form of water (CSD refcode: NAXSIQ [11], PUDGRUF [12]/PUDGRUF01 [13], SUYQAF [14], VEVNEQ [15]), ethanol (CSD refcode: AJECIB [16]) or nitrobenzene (CSD refcode: KAHMOV [17]). Interestingly, the supramolecular associations proceeding between 2-AP and benzoic acid resulted in the production of three co-crystal polymorphs described by *P*nma (CSD refcode: NUKWEW [18] and NUKWEW01 [18]) and $P2_1/n$ (NUKWOG [18]) symmetry. The conformational discrepancies observed within the group of free dichloro-substituted phenoxyacetic acid derivatives influenced into the crystal packing generated for their supramolecular adducts with 2-AP [19,20]. Inclusion of the specific isomer of dichloro-substituted phenoxyacetic derivatives caused different spatial arrangement of the structural residues included into the multi-component molecular crystals, namely *P*-1 (CSD refcode: LEWRIO [19]), $P2_1/n$ (CSD refcode: LEWREK [19]), $P2_1/c$ (CSD refcode: RADGEJ [20]) and *P*bcn (RADFEI [20]) for 3,4-, 2,4-, 2,3- and 2,6-dichlorophenoxyacetic units, respectively.

The greatest structural diversity of 2-A-4,6-DMP (Figure 2B) based supramolecular associations is demonstrated in relation to p-xylylene-bis(thioacetic) acid resulting in orthorhombic *C*mca (CSD refcode: BOQNUS [21]) and monoclinic $P2_1/c$ (CSD refcode: BOQNIG [21]) true co-crystals as well as monoclinic $P2_1/c$ (CSD refcode: BOQNOM [21]) co-crystal monohydrate containing only the neutral N–H···O and O–H···N H-bonds. The 2-A-4,6-DMP is characterized by the most flexible behavior towards carboxylic acids, so that as many as four-component crystalline solids are created. The 2-A-4,6-DMP and carboxylic co-formers present in the crystal lattices of the produced four-component supramolecules adopt the different residue type. The four-component co-crystal solvate formed between 2-A-4,6-DMP and ferulic acid (CSD refcode: JACCIC [22]) with participation of acridine and acetonitrile as solvent contains all four structural units in their starting neutral figure. In the asymmetric unit of the other four-component crystal generated from 2-A-4,6-DMP and 2-hydroxy-6-napthoic acid (CSD refcode: VAJQAB [23]) besides one water molecule, the 2-A-4,6-DMP$^+$ monocation as well as both the monoanionic and neutral form of 2-hydroxy-6-napthoic acid specie is also observed. The reverse content of acidic:basic residues, found in the molecular structure of four-component solid fabricated from 2-A-4,6-DMP and 5-aminoisophthalic acid (CSD refcode: POVXEG [24]), existed as the salt co-crystal hemihydrate which consists of a half of water molecule, one monoanion of acidic component as well as both the monocationic and neutral form of basic ingredient.

In 73,7 % of the published cases (Figure 2B), 2,4,6-triaminopyrimidine agent interact with carboxylic co-formers mostly by accepting the acidic proton by N-heterocyclic nitrogen atom and became the 2,4,6-TAP$^+$ cation. The 2,4,6-TAP$^+$ residues in these crystals are always sustained with complementary carboxylates via the charged-assisted N^+–H···O^- and multiple N–H···O^- H-bonds giving the supramolecular conglomerates in the form of salt solvates/hydrates (CSD refcode: CALVES [8,9], EPUQAK [25], KEVLUV [26], VEXQEX [27], VEXQOH [27], VEXQUN [27], VEQZOQ [27], VEXZUW [27] and VEYBAF [27]) and true salts (CSD refcode: DARMIV [28], TESRAM [29], VEYBEJ [27], VIPZUS [8,9] and YUKVAE [30]). The 2,4,6-TAP also interacts with the acidic components only by the neutral O–H···N/N–H···O H-bonds confirming the lack of proton transfer from the carboxylic species to 2,4,6-TAP entity (Figure 2B). The neutral H-bonds were observed in several 2,4,6-TAP:carboxylic SOFs appearing in the form of true co-crystal (CSD refcode: SOVNIA [31]) or co-crystal solvates/hydrates (CSD refcode: SOVLAQ [31], SOVMOF [31], SOVQAV [31], SOVQEZ [31]).

The acidic HBTA component, namely (benzylthio)acetic acid [32], owing to its chemical structure (Figure 1) containing –COOH group, organic sulphide –S– unit, –CH_2– spacers as well as aryl core seems to be excellent under non-covalent contacts. So far, HBTA was exploited only in the construction of five supramolecular conglomerates (Figure 2A) with proline compounds (CSD refcode: XITMEW [33], XITMIA [33] and XITMOG [33]) isonicotinamide (CSD refcode: XITMUM [33]) as well as tryptamine (CSD refcode: XITNAT [33]). The designated X-ray crystal structures of HBTA based supramolecular frameworks show that the acidic ingredient takes either a neutral or monoanion form (Figure 2B).

This paper is devoted to successful supramolecular self-assembly explained by the non-covalent interactions formed between the (benzylthio)acetic acid and the selected aminopyrimidines, such as 2-aminopyrimidine, 5-aminopyrimidine, 2-amino-4,6- dimethylpyrimidine and 2,4,6-triaminopyrimidine, carried out through solution co-crystallization. This work also aims to characterize the generated organic complexes in the structural and supramolecular aspects utilizing the SC X-ray crystallography as well as to determine their spectral and thermal behavior applying the FT-IR spectroscopy and thermal analysis as well. Moreover, the incorporation of 5-aminopyrimidine co-former into the process of supramolecular association with HBTA contributed to obtaining the 5-AP:carboxylic multi-component crystalline phase for the first time.

2. Materials and Methods

The co-formers and solvents used in co-crystallization experiments were commercial products without further purification. (Benzylthio)acetic acid (purity 97 %) was sourced from Sigma-Aldrich. 2-Aminopyrimidine and 5-aminopyrimidine of analytical grade were purchased from Fluorochem Ltd.. 2-Amino-4,6-dimethylpyrimidine (purity 98%) was received from Alfa Aesar GmbH, whereas 2,4,6-triaminopyrimidine (purity 97 %) was procured from Acros Organics B.V.B.A.. The short-chained alcohols (methanol and ethanol) were provided by Avantor Performance Materials Poland S.A. (formerly POCH S.A.).

2.1. Single crystal preparation by solution co-crystallization

The crystals of novel multi-component molecular materials **1-4** were afforded under solution co-crystallization based on slow solvent evaporative method at ambient conditions. The well-shaped single crystals of new supramolecular complexes were successfully harvested in co-crystallization trials, in which the equimolar amounts of particular acidic and basic co-formers were combined with each other and methanol or ethanol was applied as a solvent.

All SOFs were synthesized according to the same general procedure: a methanol or ethanol solution (5 ml) of HBTA (0.182 g, 1 mmol) was combined with the methanol or ethanol solution containing dissolved 1 mmol of individual N-containing specie (0.095 g of 2-AP and 5-AP, 0.123 g 2-A-4,6-DMP or 0.125 g of 2,4,6-TAP) and stirred for 5 min. The resulting mixtures were then left undisturbed to evaporated naturally at ambient temperature. Then, after several days, the well-shaped single crystals suitable for SC XRD analysis, were harvested. The physical parameters of grown single crystals, like colour, shape and crystal size, are gathered in Table 1.

Adduct [2-AP·HBTA] (1)

Yield for **1**: 0.251 g (90.61 %); Elemental analysis results for [$C_4H_5N_3$·$C_9H_{10}O_2S$] (MW: 277.34 g mol^{-1}). Calcd (%): C, 56.30; H, 5.45; N, 15.15; S, 11.56. Found (%): C, 56.61; H, 5.34; N, 15.28; S, 11.39.

Architecture [0.5(5-AP)·HBTA] (2)

Yield for **2**: 0.228 g (82.31 %); Elemental analysis results for [0.5($C_4H_5N_3$)·$C_9H_{10}O_2S$] (MW: 229.78 g mol^{-1}). Calcd (%): C, 57.50; H, 5.48; N, 9.14; S, 13.95. Found (%): C, 57.32; H, 5.57; N, 9.31; S, 14.06.

Association [2-A-4,6-DMP·HBTA] (3)

Yield for **3**: 0.285 g (93.44 %); Elemental analysis results for [$C_6H_9N_3$·$C_9H_{10}O_2S$] (MW: 305.39 g mol^{-1}). Calcd (%): C, 58.99; H, 6.27; N, 13.76; S, 10.50. Found (%): C, 59.17; H, 6.15; N, 13.62; S, 10.74.

Assembly [2(2,4,6-TAP$^+$)·2(BTA$^-$)·MeOH] (4)

Yield for **4**: 0.269 g (87.62 %); Elemental analysis results for [2($C_4H_8N_5$)·2($C_9H_9O_2S$)·CH_4O] (MW: 646.79 g mol^{-1}). Calcd (%): C, 50.14; H, 5.92; N, 21.66; S, 9.91. Found (%): C, 50.02; H, 5.81; N, 21.84; S, 10.08.

2.2. Single-crystal X-ray diffraction

An Oxford Diffraction Xcalibur CCD diffractometer (Oxford Diffraction Ltd., Abington, UK) equipped with graphite-monochromated MoK$_\alpha$ radiation source (λ = 0.71073 Å) was employed to collect the single crystal diffraction data for suitable selected crystals of complexes **1**-**4**. The SC XRD measurements were carried out either at low-temperature conditions (100(2) or 120(2) K) or at ambient temperature (295(2) K). The data sets were gathered using the ω scan technique with an angular scan width of 1.0 °. The *CrysAlis Pro* [34] program was used for data acquisition, cell refinement, data reduction and multi-scan absorption correction. The structures were solved by direct methods with *SHELXS*-86 [35] and refined on F^2 by full-matrix least-squares techniques with *SHELXL*-2018/3 [36] both implemented in *WinGX 2021.1* [37] software. Non-hydrogen atoms were refined with anisotropic displacement parameters. Hydrogen atoms were positioned geometrically (for carbon atoms) and were located from the different Fourier map (for oxygen and nitrogen heteroatoms) and refined as riding atoms with isotropic displacement parameters. The molecular and crystal structures graphics were presented owing to The *Mercury 2022.3.0* program [38].

CCDC 2304064–2304067 contains the supplementary crystallographic data for this paper. The summary of crystal data, experimental details and refinement results of structures in question are summarized in Table 1, whereas the geometry of intermolecular interactions existing in the crystals **1**-**4** are shown in Table 2.

Table 1. Summary of X-ray crystallographic data for co-crystals **1**-**3** and salt solvate **4**.

Compund	**1** [2-AP·HBTA]	**2** [0.5(5-AP)·HBTA]	**3** [2-A-4,6-DMP·HBTA]	**4** [2(2,4,6-TAP$^+$)·2(BTA$^-$)·MeOH]
Chemical formula	[$C_4H_5N_3$·$C_9H_{10}O_2S$]	[$C_2H_{2.5}N_{1.5}$·$C_9H_{10}O_2S$]	[$C_6H_9N_3$·$C_9H_{10}O_2S$]	[2($C_4H_8N_5^+$)·2($C_9H_9O_2S^-$)·CH_3OH]
Formula weight	277.34	229.78	305.39	646.79
T [K]	120(2)	100(2)	295(2)	120(2)
Crystal system	triclinic	monoclinic	triclinic	triclinic
Space group	*P-1*	*I*2/a	*P-1*	*P-1*
a [Ĺ]	5.473(2)	11.2873(8)	7.3644(9)	11.9766(12)
b [Ĺ]	8.720(3)	9.1219(6)	8.2883(10)	12.2477(11)
c [Ĺ]	14.262(4)	22.7196(17)	13.5264(12)	12.7081(12)

α [°]	83.08(3)	90.00	82.748(9)	99.661(8)
β [°]	82.62(3)	103.110(7)	87.375(9)	111.581(9)
γ [°]	80.40(3)	90.00	75.153(10)	106.054(8)
V [Ĺ^3]	662.1(4)	2278.3(3)	791.60(16)	1588.2(3)
Z	2	8	2	2
$D_{calc.}$ [g cm^{-3}]	1.391	1.340	1.281	1.352
μ [mm^{-1}]	0.246	0.267	0.212	0.221
Crystal colour and shape	colorles plate	colorles plate	colorles plate	colorles block
Crystal size [mm]	0.21×0.56×0.02	0.23×0.55×0.05	0.58×0.52×0.18	0.11×0.20×0.31
θ range [°]	2.895–27.477	2.902–27.485	2.560–27.485	2.582–27.484
$F(000)$	292	968	324	684
Reflections				
measured	5060	8584	6170	13063
unique	3040	2607	3637	7280
Observed data [$I > 2\sigma(I)$]	2382	2252	2317	4470
R_{int}	0.0274	0.0263	0.0324	0.0592
Completeness to θ_{max}	0.999	0.999	0.999	0.999
Goodness-of-fit on F^2	1.017	1.048	1.034	1.017
R_1, wR_2 [$I>2\sigma(I)$]	0.0421, 0.0906	0.0313, 0.0752	0.0534, 0.1299	0.0672, 0.1158
R_1, wR_2 (all data)	0.0621, 0.1023	0.0391, 0.0799	0.0893, 0.1528	0.1250, 0.1417
Residual density [e Å^{-3}]	0.289, -0.252	0.264, -0.271	0.305, -0.204	0.345, -0.326
Deposition no	2304064	2304065	2304066	2304067

Table 2. Hydrogen-bond parameters of co-crystals **1-3** and salt solvate **4**.

D–H···A*	D–H [Å]	H···A [Å]	D···A [Å]	D–H···A [°]	*Symmetry code for A
[2-AP·HBTA] (**1**)					
O2–H1O2···N1	0.96(3)	1.65(3)	2.595(2)	169(3)	x, y+1, z
N3–H1N3···O1	0.91(2)	2.09(3)	2.978(2)	167(2)	x, y-1, z
N3–H2N3···N2	0.82(2)	2.27(2)	3.090(3)	176(2)	-x-1, -y+1, -z+1
C13–H13···O2	0.93	2.66	3.531(3)	157.1	-x+1, -y+1, -z+1
[0.5(5-AP)·HBTA] (**2**)					
O1–H1O1···N1	0.90(2)	1.74(2)	2.6361(14)	176(2)	x, y-1, z
N2–H1N2···O2	0.847(16)	2.268(17)	3.0225(16)	148.6(15)	
C10–H10···O2	0.93	2.56	3.2693(17)	133.1	x, y+1, z
C10–H10···O2	0.93	2.56	3.2693(17)	133.1	-x+3/2, y+1, -z
C11–H11···S1	0.93	2.84	3.7208(13)	158.5	
[2-A-4,6-DMP·HBTA] (**3**)					
O2–H1O2···N1	1.01(3)	1.64(3)	2.645(2)	170(3)	
N3–H1N3···O1	0.81(2)	2.11(3)	2.916(3)	172(2)	
N3–H2N3···N2	0.83(2)	2.20(2)	3.036(3)	177(2)	- x-1, -y+2, -z+1
C3–H3A···O2	0.97	2.54	3.249(3)	129.5	
[2(2,4,6-TAP$^+$)·2(BTA$^-$)·MeOH] (**4**)					
N2–H1N2···O4	0.95(3)	1.74(4)	2.684(3)	176(3)	-x-1, -y+1, -z
N7–H1N7···O2	0.93(4)	1.80(4)	2.724(3)	173(3)	-x-1, -y, -z
N3–H2N3···O2	0.90(3)	2.24(3)	3.028(3)	146(2)	x-1, y, z

N4–H1N4···O3	0.85(4)	1.99(4)	2.842(4)	179(3)	-*x*-1, -*y*+1, -*z*
N4–H2N4···O1	0.83(3)	2.10(3)	2.906(4)	164(3)	
N5–H2N5···O2	0.94(3)	2.03(4)	2.921(3)	158(3)	-*x*, -*y*, -*z*+1
N8–H1N8···O4	0.89(4)	2.07(4)	2.957(3)	176(3)	-*x*-1, -*y*+1, -*z*
N8–H2N8···O1	0.95(3)	1.91(3)	2.853(4)	169(3)	-*x*-1, -*y*, -*z*
N9–H2N9···O3	0.85(4)	2.03(4)	2.877(3)	173(4)	-*x*-2, -*y*+1, -*z*
N3–H1N3···N6	0.82(4)	2.23(4)	2.947(4)	146(3)	
N5–H1N5···N1	0.84(3)	2.41(3)	3.147(4)	146(3)	-*x*-1, -*y*, -*z*+1
N9–H1N9···N3	0.83(3)	2.48(4)	3.249(4)	155(3)	-*x*-2, -*y*, -*z*
N10–H2N10···O5	0.89(3)	1.98(3)	2.835(4)	161(3)	*x*-1, *y*, *z*
N5–H1N5···S2	0.84(3)	2.91(3)	3.534(3)	133(3)	-*x*-1, -*y*+1, -*z*+1
O5–H1O5···S1	0.75(5)	2.56(5)	3.297(3)	165(4)	
C12–H12···S1	0.93	2.81	3.646(3)	150.5	

2.3. Instrumentation and measurement methodology

A Perkin Elmer 2400 Series II CHNS/O elemental analyzer (PerkinElmer Inc., Waltham, USA) operating with the CHNS mode was employed to determine the percentage contents of carbon, hydrogen, nitrogen and sulphur in adducts **1**-**4**.

A SETSYS 16/18 (Setaram, Caluire, France) thermal apparatus registering the TG and DSC thermal curves was used to measure the thermal behavior of complexes **1**-**4** as well as the thermal properties of individual molecular components. Weighted samples (7.085–8.692 mg) were placed in the alumina crucibles and scanned from 30 to 800 °C. The TG/DSC measurements were conducted under the dynamic air atmosphere (at the rate of the airflow of 0.75 dm^3 h^{-1}) with a constant heating rate of 10 °C min^{-1}.

A FT/IR-4600 (JASCO Corporation, Tokyo, Japan) Fourier-transform infrared spectrometer was utilized to receive the transmission infrared spectra of all the starting molecular ingredients and co-crystallization products as well. The spectra of the tested compounds in the region 4000–400 cm^{-1} were recorded as pressed disks in the KBr matrix.

3. Results and Discussion

The four novel supramolecular organic frameworks based on (benzylthio)acetic acid (HBTA) and selected aminopyrimidines as co-formers (Figure 1) were profitably received in the form of good X-ray quality single crystals. The well-shaped single crystals of multi-component molecular materials **1**-**4** were grown by utilizing the solution co-crystallization relied on the natural evaporating method according to the preparation scheme and synthesis details presented in Figure 3 and in the Materials and Methods section, respectively. The prepared SOFs are characterized by different stoichiometry despite the inclusion of the same molar ratios of starting molecular entities in co-crystallization. Only in the case of adduct **4** formed from HBTA and 2,4,6-TAP, one MeOH solvent molecule is incorporated into the crystal lattice. The co-crystallization products were also investigated by means of FT-IR spectroscopy as well as thermal analysis in air to support the results gained from SC XRD structural study.

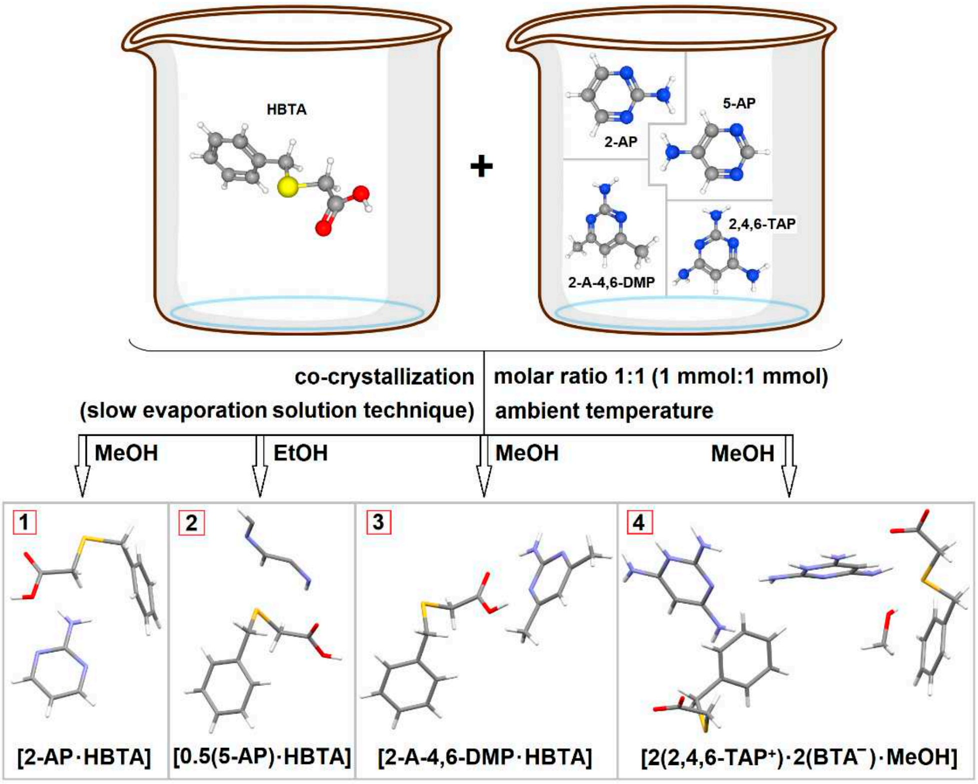

Figure 3. The preparation scheme for crystalline solids **1**-**4**.

3.1. Structural and Supramolecular Characteristics

The aminopyrimidine based supramolecular complexes **1**-**4** were defined as [2-AP·HBTA] (**1**), [0.5(5-AP)·HBTA] (**2**), [2-A-4,6-DMP·HBTA] (**3**) and [2(2,4,6-TAP^{+})·2(BTA^{-})·MeOH] (**4**). The disclosed compositions of the residues present in the crystal lattices indicate that the isolated crystals belong to two different forms distinguished upon the classification procedure of multicomponent crystalline phases [10], that is true co-crystal (architectures **1**-**3**) and salt solvate (adduct **4**).

3.1.1. True co-crystal obtained from 2-AP and HBTA (1)

Compound **1** crystallizes in a triclinic crystal system in *P-1* space group (Table 1). The atom numbering and the conformation of **1** in the crystal are shown in Figure 4. The asymmetric unit of **1** consists of one (benzylthio)acetic acid (HBTA) and one 2-aminopyrimidine (2-AP) molecule. The C1–O1 and C1–O2 bond lengths of acid molecule are equal 1.217(3) Å and 1.309(3) Å respectively, indicating that the hydrogen atom is located on the O2 atom (Figure 4A). The pyrimidine ring lies almost in the same plane as the alkyl chain of acid molecule, whereas the dihedral angle between the plane of the phenyl ring of HBTA molecule and the pyrimidine moiety of 2-AP is 116.2 ° (Figure 4B).

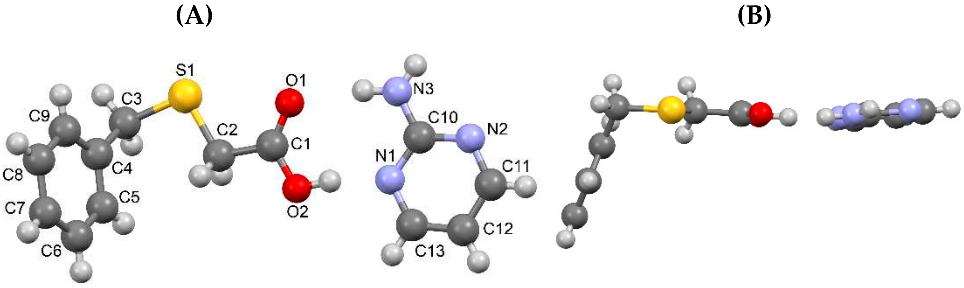

Figure 4. The molecular structure of **1** showing the atom-labelling scheme (**A**) and the orientation of the phenyl ring of acid molecule in respect to pyrimidine moiety (**B**).

The primary hydrogen bonding observed in [2-AP·HBTA] co-crystal is an aminopyrimidine···acid dimer (Figure 5). This $R_2^2(8)$ heterodimer is formed by O2–H···N1 and N3–H···O1 hydrogen bonds (Donor···Acceptor distances and D–H···A angles are given in Table 2). Such dimers are connected alternately by two synthons: N3–H···N2 hydrogen bond and C13–H···O2 interaction (Figure 5). Both synthons result in the formation of two further ring motifs: homomeric ring $R_2^2(8)$ formed by N3–H···N2 bond and a tetramer based upon a centrosymmetric $R_4^4(10)$ motif based on C13–H···O2 contact and O2–H···N1 hydrogen bond. All these synthons result in the formation of a stable ribbon presented in Figure 5.

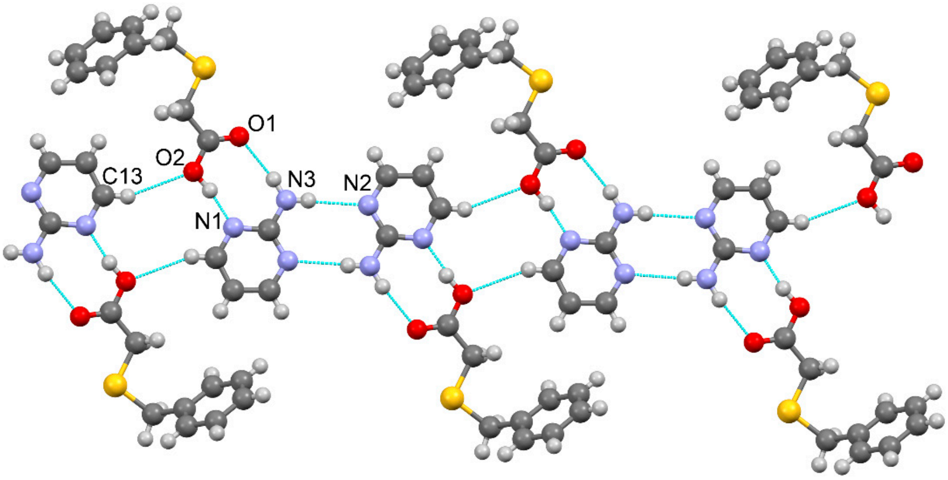

Figure 5. H-bond synthons in the crystal lattice of **1**.

3.1.2. Real co-crystal formed between 5-AP and HBTA (2)

Compound **2** crystallizes in the monoclinic *I*2/a space group (Table 1) with one molecule of (benzylthio)acetic acid (HBTA) and a half molecule of 5-aminopyrimidine (5-AP) in the asymmetric unit. The C1–O1 bond length is equal 1.322(2) Å, being longer than C1–O2 bond (1.210(2) Å), which proves the localization of hydrogen atom on the O1 atom of acid molecule (Figure 6A). The conformation of alkyl sulfanyl chain of HBTA molecule in co-crystal with 5-aminoaminopyrimidine (**2**) differs from its planar architecture in co-crystal with 2-aminoaminopyrimidine (**1**) (Figures 4B and 6B). The torsional angle C3–S1–C2–C1 is equal -68.8(1)° for compound **2**, whereas for compound **1** it was -179.1(1)°. The pyrimidine moiety of compound **2** lies almost in the same plane as the S1–C2–C1 chain of acid molecule and the dihedral angle between the plane of the phenyl and pyrimidine rings is 46.1 °.

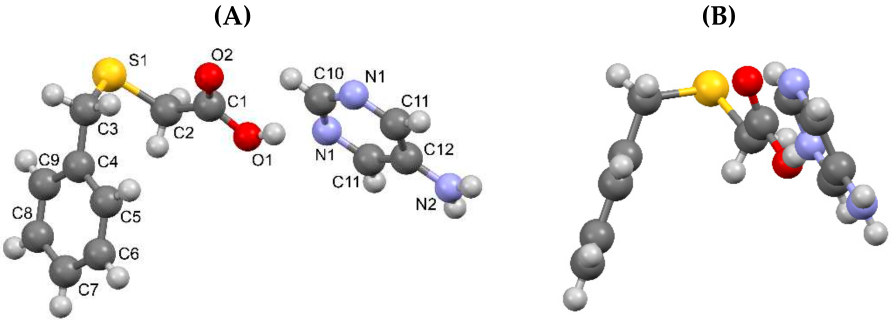
(A) **(B)**

Figure 6. The molecular structure of **2** presenting the atom-labelling scheme **(A)** and the orientation of the phenyl ring of acid molecule in respect to pyrimidine moiety (**B**).

The molecule of (benzylthio)acetic acid is bonded to two 5-aminopyrimidine molecules resulting in the formation of two types of dimers: $R_2^2(9)$ and $R_2^2(8)$ (Figure 7). The $R_2^2(9)$ dimer is formed by

N2–H···O2 and C11–H···S1 contacts (Table 2), and 5-AP molecule act as donor and HBTA molecule become hydrogen bond acceptor. The second dimer, described with $R_2^2(8)$ graph-set motif, is formed through O1-H···N1 and C10–H···O2 interactions. In this dimer, both components act as hydrogen bond donors and acceptors. Both dimers, repeated with a two-fold axis passing through the pyrimidine rings, form a tetramer. The 5-AP molecules link such tetramers in a strong ribbon-like structure (Figure 7).

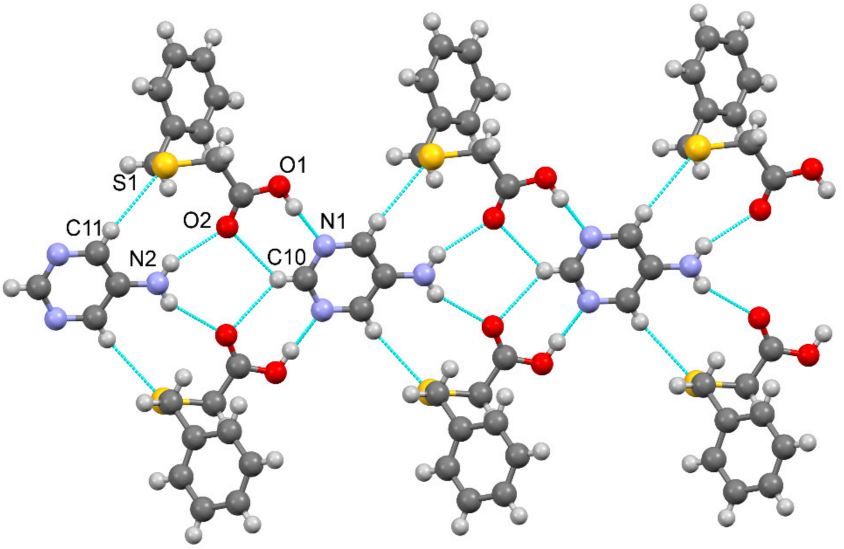

Figure 7. H-bond synthons in the crystal lattice of **2**.

3.1.3. True co-crystal based on 2-A-4,6-DMP and HBTA (3)

The crystal structure analysis of **3** reveals a 1:1 co-crystal that crystallizes in the triclinic *P-1* space group (Table 1). The asymmetric part of **3** consists of one neutral molecule of (benzylthio)acetic acid (HBTA) acid and one neutral molecule of 2-amino-4,6-dimethylpyrimidine (2-A-4,6-DMP). The length of the C1–O1 and C1–O2 bonds are 1.211(2) Å and 1.303(3) Å, respectively, indicating that the H atom is located on the O2 atom of acid molecule (Figure 8A). The torsional angle C3–S1–C2–C1 in HBTA is -84.9(2) °. Such stereochemistry of the alkyl sulfanyl chain of acid molecule causes the formation of C3–H···O2 intramolecular hydrogen bond. The phenyl part of HBTA and the pyrimidine ring are approximately perpendicular to each other (Figure 8B), the value of dihedral angle between the planes formed by these moieties is 76.5 °.

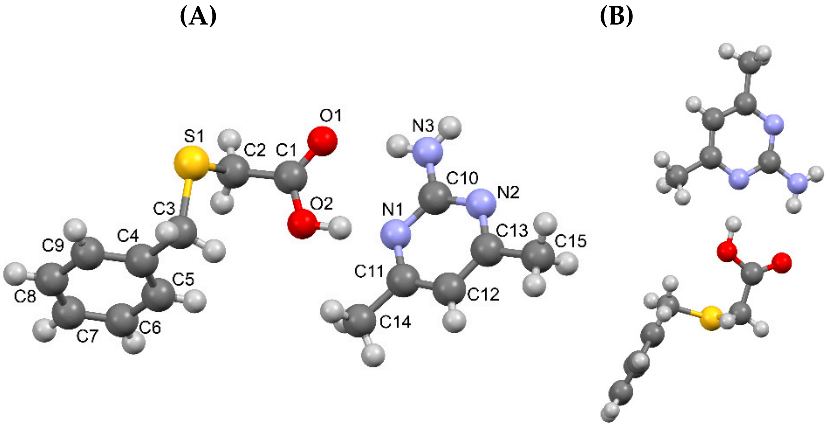

Figure 8. The asymmetric unit of **3** showing the atom-labelling scheme (**A**) and the orientation of the phenyl ring of acid molecule in respect to pyrimidine moiety (**B**).

The carboxyl group of HBTA and 2-A-4,6-DMP molecule act as donor and acceptor of hydrogen bond forming $R_2^2(8)$ heterodimer through O2–H···N1 and N3–H···O1 contacts (Figure 9, Table 2). Such synthon is similar to dimer motif observed in co-crystal **1**, what is related to the presence of $-NH_2$ group at C10 of the pyrimidine ring. Two 2-A-4,6-DMP molecules in co-crystal **3** are linked via the N3–H···N2 hydrogen bonds and the formation of centrosymmetric homomeric $R_2^2(8)$ dimer is observed. All described synthons build a tetrameric supramolecular unit are presented in Figure 9.

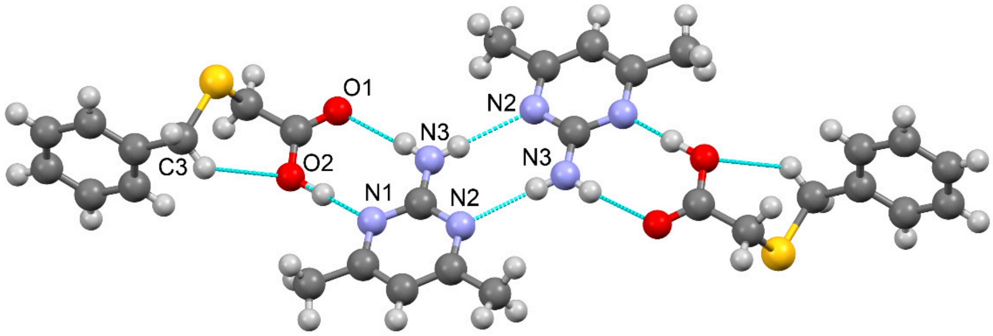

Figure 9. H-bond synthons in the crystal lattice of **3**.

3.1.4. Salt methanol solvate derived from 2,4,6-TAP and HBTA (4)

Compound **4** crystallizes in the triclinic *P-1* space group (Table 1). 2,4,6-Triaminopyrimidine (2,4,6-TAP) forms a 2:2:1 molecular adduct with (benzylthio)acetic acid (HBTA) and solvent. However, proton transfer occurs generating a salt, not a co-crystal as in the case of the compounds containing monoaminopyrimidine component (compounds **1**-**3**). The asymmetric unit of **4** consist of two (benzylthio)acetate anions (BTA^-), two 2,4,6-triaminopyrimidinium (2,4,6-TAP^+) cations and one methanol molecule (Figure 10). The bond length C1–O1/O2 and C14–O3/O4 are equal 1.240(4)/1.277(5) Å and 1.246(4)/1.269(5) Å, respectively that confirms the deprotonation of acid molecules. The stereochemistry of alkyl chains differ between two acid anions – torsional angles C3–S1–C2–C1/C16–S2–C15–C14 are 174.9(3)/78.7(3)°.

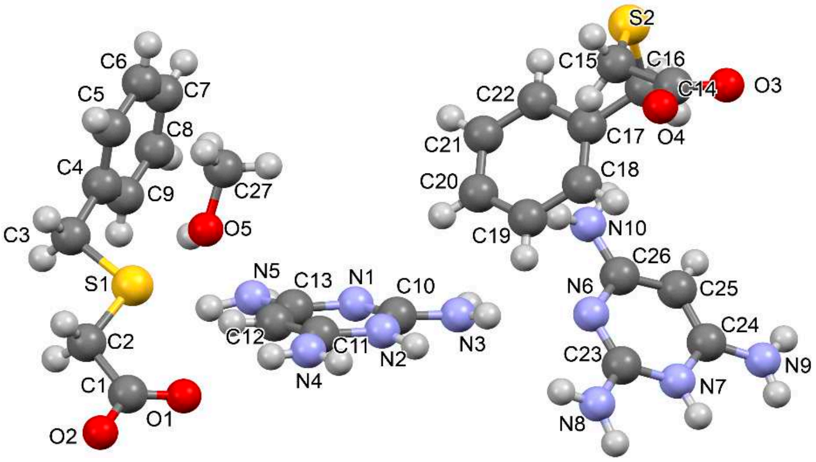

Figure 10. The asymmetric unit of **4** showing the atom-labelling scheme.

The crystal structure analysis of **4** revealed the presence of as many as 10 types of N–H···O, three types of N–H···N and one type of N/O/C–H···S synthons, presented in detailed in Table 2. Such very complex hydrogen-bonding scheme, arising from the superabundance of donors and acceptors, lead to the formation of stable 3-D structure presented in Figure 11.

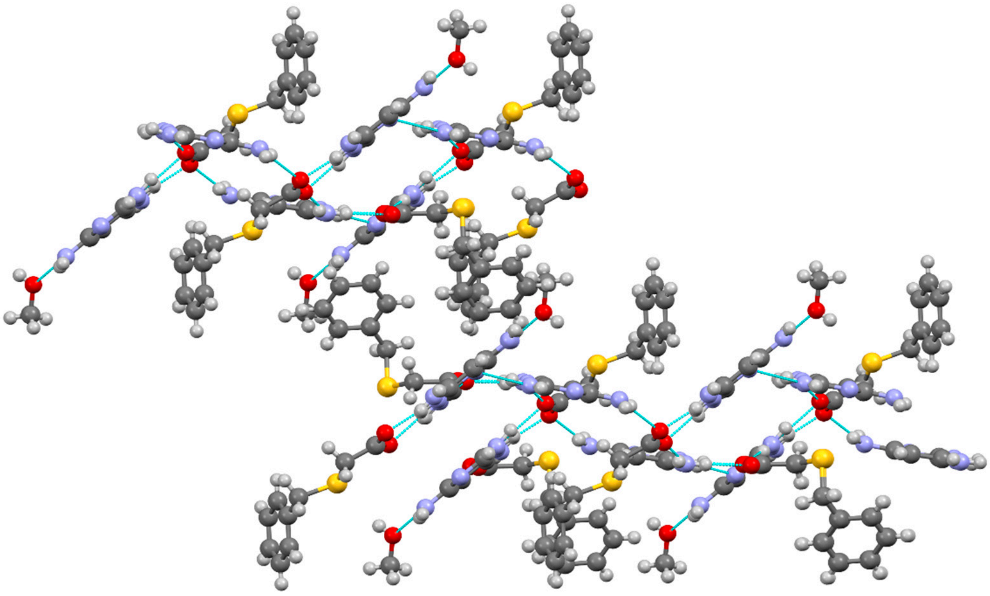

Figure 11. H-bond synthons in the crystal lattice of **4**.

3.2. Thermal behavior in air atmosphere

The novel crystalline solids were investigated through thermal analysis based on the thermogravimetry (TG) combined with the differential scanning calorimetry (DSC) in order to establish their composition and thermal behavior under the controllable heating. The summary of the TG and DSC courses for supramolecular complexes **1**-**4** against the TG and DCS traces of corresponding molecular components are presented in Figures 12 and 13, respectively. As follows from Figures 12 and 13, all supramolecular materials are characterized by different courses of their thermal traces in relation to the thermal curves for starting co-partners, which clearly indicate the formation of novel multi-component crystalline phases.

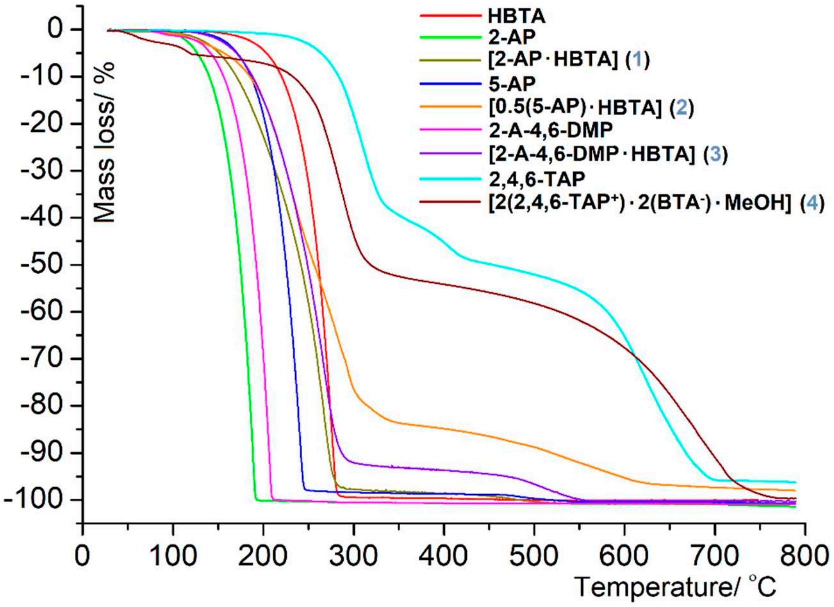

Figure 12. The TG profiles of supramolecular adducts **1**-**4** along with the TG curves of suitable molecular building bricks.

The supramolecular complexes **1**-**3** are unsolvated solids being thermally stable up to about 108 °C , 109 °C and 135 °C, respectively, as indicated by the platou visible on their TG profiles in the above temperature ranges. The Complex **4** is stable at room temperature and was defined as monosolvate. In the case of conglomerate **4**, the desolvation proces takes place in one stage above 40 °C. The removal of MeOH molecule corresponding to the first weight loss of 5.16 % found on the TG plot up to 132 °C, which coincided with the theoretical value of 4.95 %. The release of MeOH molecule is also echod with the first detectable endothermic effect seen on DSC curve with the peak top located at 83 °C indicating the lower stability for heat of salt solvate against co-crystals. The higher temperature of MeOH liberation exhibited by complex **4** compared to the boiling point of pure MeOH suggests the interaction of methanol molecule with co-partners residues through intermolecular H-bonds. After the loss of MeOH molecule, the unstable product in the form of the unsolvated salt begins to decompose immediately up to 750 °C along with the burning of cationic and anionic residues in two evident steps. Each of the two stages of combustion of the ions is associated with an identical mass loss (found: 47.42 %; calcd.: 47.52 %), which indicates that in each decomposition stage one TAP^+ and one BTA^- residue from assymetric unit are burned. The first stage of exothermic decomposition, proceding between 132 °C and 330 °C, is connected only with the combustion of those TAP^+ and BTA^- species that formed H-bonds with MeOH, whereas the second exotermic degradation step, going from 132 °C to 750 °C, is associated with the burning of those ionic residues that were not H-bonded to the solvent, which is consistent with the crystal structure of salt solvate **4**. Further heating above the level of thermal resistance of co-crystals **1**-**3** causes the explosion of all base and acidic components up to about 538 °C, 648 °C and 570 °C, respectively, reflected by several exothermic peaks situated on their DSC traces. The strongest heat releases during decomposition process are visible on DSC profiles as most intense exothermic maxima located nearby 477 °C (**1**), 526 °C (**2**), 503 °C (**3**) and 668 °C (**4**). The characteristically sharp and single peak seen in each DSC thermogram reflects the endothermic effect of the melting process of given compound. The unsolvated forms of adducts, namely [2-AP·HBTA] (**1**), [0.5(5-AP)·HBTA] (**2**), [2-A-4,6-DMP·HBTA] (**3**) and [2(2,4,6-TAP^+)·2(BTA^-)] (**4**), melt before the exothermic degradations of co-partners residues. The melting points of associations **1**-**4** have distinct values (87 °C (**1**), 96 °C (**2**), 105 °C (**3**) and 125 °C (**4**)) than the melting points of starting ingredients (64 °C (HBTA) [32], 127 °C (2-AP) [13], 173 °C (5-AP), 153 °C (2-A-4,6-DMP) [21] and 248 °C (2,4,6-TAP)), which clearly proves the formation of novel crystalline solids without phase impurity. The melting points of adducts **1**-**4** lie between the melting points of corresponding co-partners which is typical for binary crystals. Finally, all crystals decompose with aproximately 100 % sample weights converted into the gasous decomposition products.

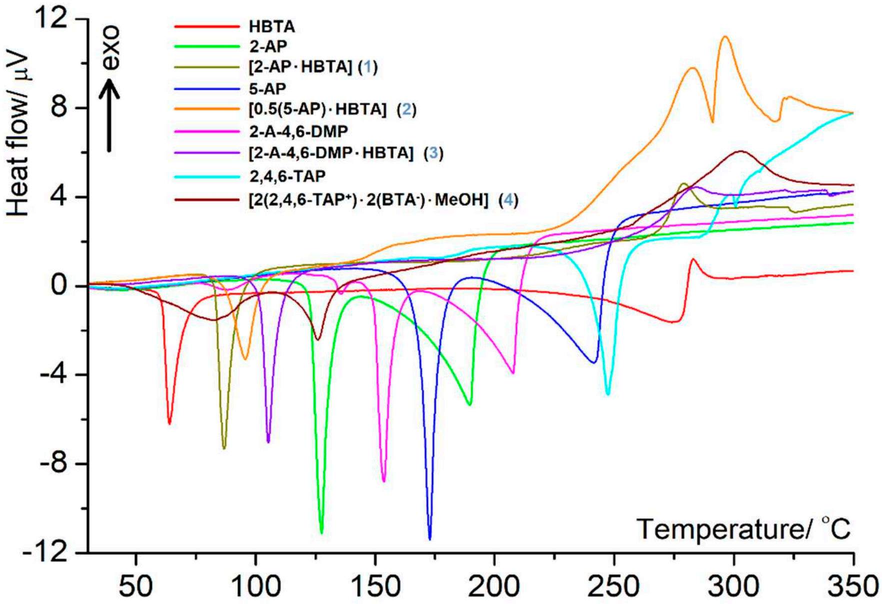

Figure 13. The DSC curves of supramolecular assemblies **1**-**4** in comparison to DSC plots of the molecular components between 30 and 350 °C.

3.3. FT-IR Characteristics

FT-IR spectroscopy is a significant technique for characterizing crystalline solids in terms of distinguishing co-crystals or salts, especially when one of the co-partner is a carboxylic derivative. The determination of multi-component crystalline phases in co-crystal/salt category is based on the identification of functional groups within the molecular co-partners embodied into the supramolecular complexation process. The FT-IR spectra of starting ingredients and their ground mixtures are illustrated in Figures 14 and 15. The spectral traces recorded for phases **1**-**4** show that both the acidic and suitable basic residues are present in the tested solids, but the supramolecular complexation between them through intermolecular contacts resulted in shifting of characteristic stretching vibrational modes derived from the starting co-partners. The formation of these new multi-component solid forms is especially displayed by shifting of stretching vibrations of those functionals, like –COOH, –NH$_2$ as well as N-pyrimidine atom, which are the strong sites in H-bonding.

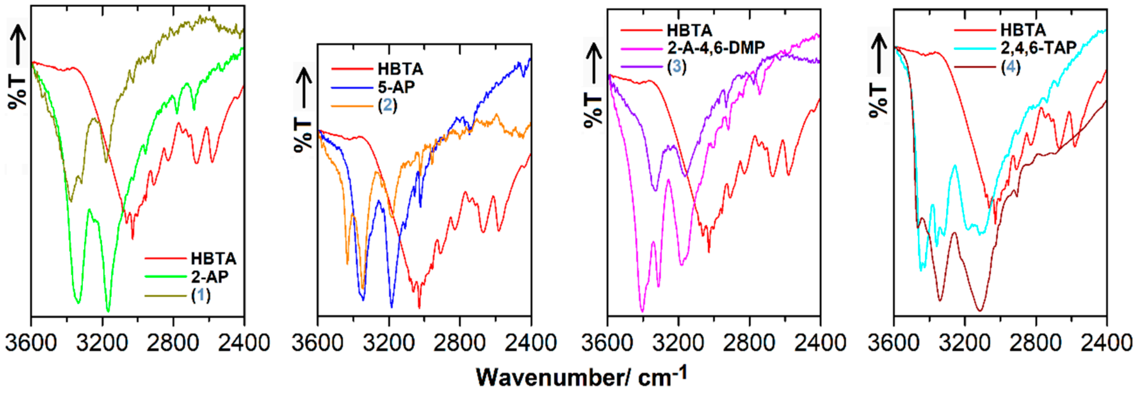

Figure 14. The comparison of infrared spectral traces in the range of 3600-2400 cm^{-1} for associations **1**-**4** as well as the free co-partners.

The HBTA molecule possesses one neutral acidic –COOH motif. The HBTA spectrum recorded in KBr matrix is dominated by the strongest absorption band at 1697 cm^{-1} [39] associated with the stretching ν(C=O) vibrational mode of carbonyl part of –COOH specie. The spectral profiles of associations **1**-**3** (Figure 15) bear this most diagnostic vibrational mode of acidic functional, but its position is slightly shifted in relation to its location in the spectrum of free HBTA ingredient. The bands of stretching ν(C=O) vibrations are observed for adducts **1**-**3** at 1692 cm^{-1} (**1**), 1707 cm^{-1} (**2**) and 1691 cm^{-1} (**3**), respectively. The presence of the absorption peaks corresponding to the ν(C=O) stretches is the most reliable proof concerning the true co-crystals formation, which coincidence with the SC X-ray data about the lack of proton transfer from the acidic co-partner to the base one during supramolecular complexation. On the other hand, the basic co-partners in the form of 2-AP, 5-AP and 2-A-4,6-DMP have only one –NH$_2$ group, which is identified by the high-energy absorption bands of asymmetric ν_{as}(NH$_2$) and symmetric ν_{s}(NH$_2$) stretching vibrations situated at 3334 cm^{-1} and 3165 cm^{-1} (3330 cm^{-1} and 3150 cm^{-1} [40]) for 2-AP, 3345 cm^{-1} and 3184 cm^{-1} for 5-AP as well as 3314 cm^{-1} and 3182 cm^{-1} (3311 and 3168 cm^{-1} [41]) for 2-A-4,6-DMP. Moreover, the spectrum of 2-A-4,6-DMP contains the strong and broadened absorption band comprising of the maximum at 3402 cm^{-1} and shoulder at 3379 cm^{-1}, which is absent after complexation with HBTA. Besides the a single-component crystal [42], the 2-A-4,6-DMP under ambient conditions may also forms a true solvate in the form of monohydrate [43]. Thus, the aforementioned frequencies are actually associated with the asymmetric and symmetric combination of stretching ν(OH) vibrations originating from incorporated water molecule. The monohydrate nature of 2-A-4,6-DMP used as co-partner in this study is also indicated on the TG and DSC thermal results (Figures 14 and 15). The visible mass loss of 1.32 % (calcd.: 1.44 %) seen on TG plot up to 106 °C supported by the endothermic effect visible on DSC curve at 88 °C clearly points to the monohydrated nature of 2-A-4,6-DMP. The ν_{as}(NH$_2$) and ν_{s}(NH$_2$) stretches of amino group derived from suitable aminopyrimidine component in the registered spectra of complexes **1**-**3** are active at 3376 cm^{-1} and 3180 cm^{-1} (**1**), 3346 cm^{-1} and 3181 cm^{-1} (**2**) as well as 3331 cm^{-}

^{1} and 3164 cm^{-1} (**3**), respectively. The spectral data concerning the $\nu_{as}(NH_2)$ and $\nu_s(NH_2)$ fundamentals found in the spectra of conglomerates **1-3** indicates that the basic ingredients remain in their original figure and they are consistent with the previously published infrared data associated with co-crystals formed between 2-AP and 1,4-cyclohexanedicarboxylic [11] or 3-nitrophthalic [44] acid as well as between 2-A-4,6-DMP and benzoic [45], indole-3-acetic [26] or butyric-3-acetic [26] acid.

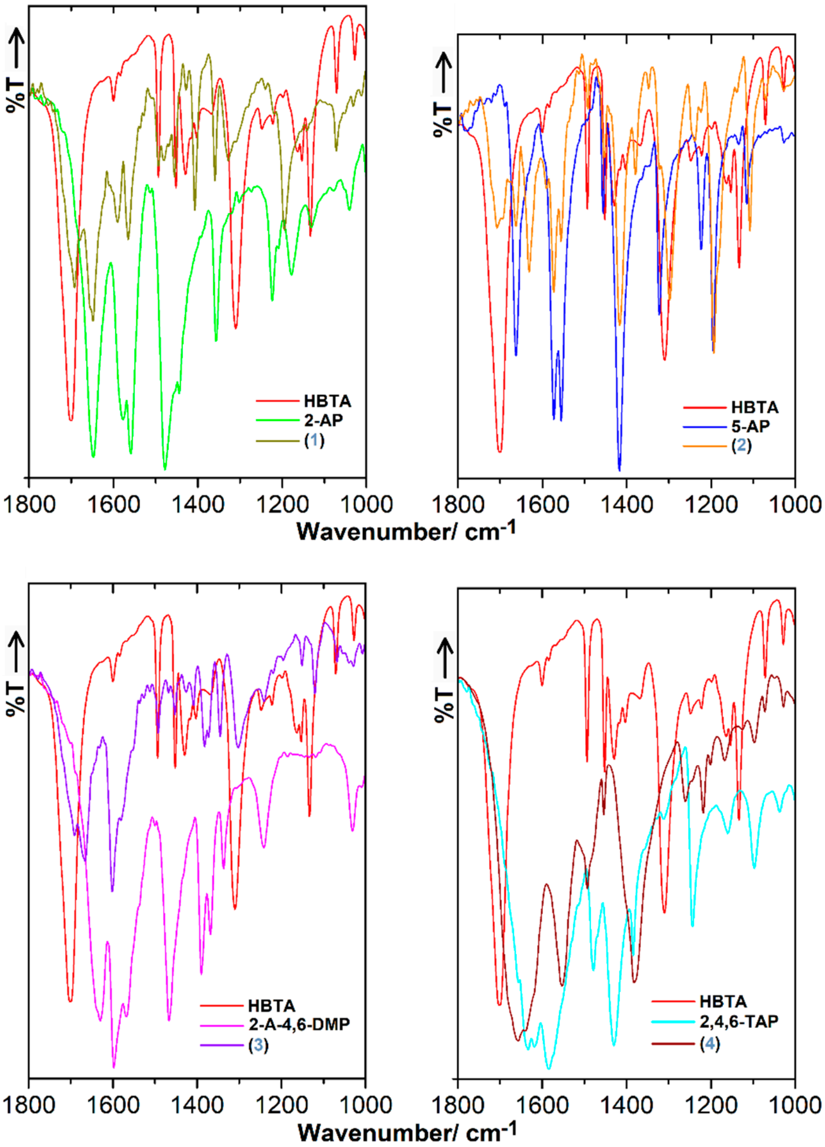

Figure 15. The FT-IR profiles for phases **1-4** in relation to the infrared plots of starting components between the region of 1800 and 1000 cm^{-1}.

The infrared spectrum of adduct **4** does not show any peak near 1700 cm^{-1} derived from the $\nu(C{=}O)$ stretching vibrational mode of original form of HBTA. Complex **4** bears two specific bands located at 1551 cm^{-1} and 1379 cm^{-1} assigned to the asymmetric $\nu_{as}(COO^-)$ and symmetric $\nu_s(COO^-)$ stretches of carboxylate group, respectively. The presence of carbxylate stretching motions instead of carbonyl stretching vibrations points to the transfer of an acidic proton from HBTA into the 2,4,6-TAP resulting in the formation of organic salt in this case. The occurrence of the co-partners only in the ionized forms is also reflected in designated X-ray crystal structure of assembly **4**. The 2,4,6-TAP contain three $-NH_2$ groups, so the numerous maxima observed in the spectrum of free 2,4,6-TAP between the 3448 cm^{-1} and 3315 cm^{-1} correspond to the asymmetric $\nu_{as}(NH_2)$ and symmetric $\nu_s(NH_2)$ stretching vibrations from amino groups (3460–3316 cm^{-1} [46]). According to the crystal structure of salt solvate **4**, it is expected that the high energetic spectral region is represent by the characteristically broadened and simultaneously overlapping bands associated with the various stretching vibrational modes (ν_{as}(NH$_2$) and ν_s(NH$_2$), ν($^+$NH) and ν(OH)) originating from those functional groups that act as strong H-bonded sites, such as the amino functionals, the pyrimidinium unit as well as the hydroxyl group of methanol, respectively.

4. Conclusions

Four novel aminopyrimidine based multi-component crystalline solids distinguished by phase purity were prepared with (benzylthio)acetic acid. The generated supramolecular assemblies with binary and tri-component conglomerate were characterized through by SC XRD, FT-IR and TG-DSC techniques. The organic binary adducts obtained from 2-AP, 5-AP and 2-A-4,6-DMP form the co-crystals, whereas the tri-component assembly fabricated with the help of 2,4,6-TAP gives the salt methanol solvate.

It is shown that aminopyrimidines are a great supramolecular moieties that generate crystals with different hydrogen bonding network. Because of the presence of N-atoms, all multi-component crystals contain strong N–H···O interaction: one type observed in three new co-crystals and ten types formed within the crystal structure of salt methanol solvate. This significant difference in the number of hydrogen bonds is related to the transfer of a proton between the acid molecule and 2,4,6-triaminopyrimidine. When hydrogen proton is transferred between the adjacent components it is easier to generate hydrogen bonds at the site of the proton transfer. Neutral molecules in co-crystals with 2-AP, 5-AP and 2-A-4,6-DMP are connected with mainly one type of O–H···N, N–H···O/N, C–H···O/S hydrogen bond, forming 1D ribbons or tetrameric unit. Sixteen type of interactions (N–H···O/N/S, O/C–H···S) observed in the crystal structure of salt solvate with 2,4,6-TAP cause the creation of stable 3-D structure.

On the other hand, the HBTA is a flexible structural fragment that efficiently creates the diversiform of supramolecular frameworks with stable H-bonded motif, making it a noteworthy molecular ingredient with high activity for co-crystal/salt formation.

Author Contributions: Conceptualization, J.S.-G.; methodology, J.S.-G.; investigation, J.S.-G.; data interpretation, J.S.-G and A.D.-A.; writing—original draft preparation, J.S.-G. and A.D.-A.; writing—review and editing, J.S.-G. and A.D.-A.; visualization, J.S.-G. and A.D.-A.; supervision, J.S.-G.; project administration, J.S-G.; funding acquisition, J.S-G.. All authors have read and agreed to the published version of the manuscript.

Funding: This research was financially supported by the National Science Centre (NCN) of Poland within the grant number 2019/03/X/ST5/01502.

Institutional Review Board Statement: Not applicable.

Informed Consent Statement: Not applicable.

Data Availability Statement: Not applicable.

Conflicts of Interest: The authors declare no conflict of interest.

References

1. Ebenezer, S.; Muthiah, P.T. Design of co-crystals/salts of aminopyrimidines and carboxylic acids through recurrently occurring synthons. *Cryst. Growth Des.* **2012**, *12*, 3766-3785.
2. Oruganti, M.; Nechipadappu, S.K.; Khade, P.A.; Trivedi, D.R. Solid-state versatility of the molecular salts/cocrystals of 2-chloro-4-nitrobenzoic acid: A case study on halogen bonds. *ACS Omega* **2017**, *2*, 7146-7162.
3. Mirzaei, M.; Sadeghi, F.; Molčanov, K.; Zaręba, J.K.; Gomila, R.M. Recurrent supramolecular motifs in a series of acid–base adducts based on pyridine-2,5-dicarboxylic acid *N*-oxide and organic bases: Inter- and intramolecular hydrogen bonding. *Cryst. Growth Des.* **2020**, *20*, 1738-1751.
4. Odiase, I.; Nicholson, C.E.; Ahmad, R.; Cooper, J.; Yufit, D.S.; Cooper, S.J. Three cocrystals and a cocrystal salt of pyrimidin-2-amine and glutaric acid. *Acta Cryst.* **2015**, *C71*, 1-8.
5. Zhang, L.; Zhou, J.; Wu, Y.; Wang, P.; Jin, S.; Lu, Y. Noncovalent-bonded 2D-3D supramolecular adducts from 6-methylpyridine-3-carboxamide and carboxylic acids. *J. Mol. Struct.* **2022**, *1264*, 133256.
6. Wu, R.; Yu, Y.; Guo, M.; Jin, S.; Wang, D. Eight salts of 4-dimethylaminopyridine and organic acids by H-bonds and some noncovalent associations. *J. Mol. Struct.* **2021**, *1230*, 129850.

7. Xu, W.; Hu, K.; Lu, Y.; Ye, H.; Jin, S.; Li, M.; Guo, M.; Wang, D. The crystal structures of ten supramolecular salts of benzylamine and organic acids. *J. Mol. Struct.* **2020**, *1219*, 128554.
8. Groom, C.R.; Bruno, I.J.; Lightfoot, M.P.; Ward S.C. The Cambridge Structural Database. *Acta Cryst.* **2016**, *B72*, 171-179.
9. Bruno, I.J.; Cole, J.C.; Edgington, P.R.; Kessler, M.; Macrae, C.F.; McCabe, P.; Pearson, J.; Taylor, R. New software for searching the Cambridge Structural Database and visualizing crystal structures. *Acta Cryst.* **2002**, *B58*, 389-397.
10. Grothe, E.; Meekes, H.; Vlieg, E.; ter Horst, J.H.; de Gelder, R. Solvates, salts, and cocrystals: A proposal for a feasible classification system. *Cryst. Growth Des.* **2016**, *16*, 3237-3243.
11. Jin, S.; Wang, D.; Liang, S.; Chen, S. Crystal and molecular structure of two organic acid–base adducts from 2-aminopyrimidine and carboxylic acids. *J. Chem. Crystallogr.* **2012**, *42*, 759-766.
12. Eshtiagh-Hosseini, H.; Yousefi, Z.; Mirzaei, M. 2-Aminopyrimidinium hydrogen oxalate monohydrate. *Acta Cryst.* **2009**, *E65*, o2816.
13. Miyan, L.; Adam, A.M.A.; Refat, M.S.; Alsuhaibani, A.M. 2-Aminopyrimidine-oxalic acid liquid-liquid charge-transfer interactions: Synthesis, spectroscopic characterizations, and the effect of temperature. *J. Mol. Liq.* **2022**, *365*, 120106.
14. Eshtiagh-Hosseini, H.; Mahjoobizadeh, M.; Mirzaei, M. 2-Aminopyrimidinium 4-hydroxypyridinium-2,6-dicacoxylate monohydrate. *Acta Cryst.* **2010**, *E66*, o2210.
15. Smith, G.; Wermuth, U.D.; Healy, P.C. Hydrogen bonding in proton-transfer compounds of 5-sulfosalicylic acid with *ortho*-substituted monocyclic hetroaromatic Lewis bases. *J. Chem. Crystallogr.* **2006**, *36*, 841-849.
16. Smith, G.; Wermuth, U.D.; Healy, P.C.; White, J.M. Structure-making with 3,5-dinitrosalicylic acid. II.* The proton-transfer compounds of 3,5-dinitrosalicylic acid with the monocyclic heteroaromatic amines. *Aust. J. Chem.* **2003**, *56*, 707-713.
17. Kobayashi, K.; Shirasaka, T.; Yamaguchi, K. Sakamoto, S.; Horn, E.; Furukawa, N. Molecular capsule constructed by multiple hydrogen bonds: self-assembly of cavitand tetracarboxylic acid with 2-aminopyrimidine. *Chem. Commun.* **2000**, 41-42.
18. Skovsgaard, S.; Bond, A.D. Co-crystallization of benzoic acid derivatives with N-containing bases in solution and by mechanical grinding: stoichiometric variants, polymorphism and twinning. *CrystEngComm* **2009**, *11*, 444-453.
19. Lynch, D.E.; Smith, G.; Freney, D.; Byriel, K.A.; Kennard, H.L.Molecular cocrystals of carboxylic acids. XV* Preparation and characterization of heterocyclic base adducts with a series of carboxylic acids, and the crystal structures of the adducts of 2-aminopyrimidine with 2,6-dihydroxybenzoic acid, 4-aminobenzoic acid, phenoxyacetic acid, (2,4-dichlorophenoxy)acetic acid, (3,4-dichloro)phenoxyacetic acid and salicylic acid, and 2-aminopyridine with 2,6-dihydroxybenzoic acid. *Aust. J. Chem.* **1994**, *47*, 1097-1115.
20. Lynch, D.E.; Barfield, J.; Frost, J.; Antrobus, R.; Simmons, J. Conformational comparisons between phenoxyacetic acid derivatives in adducts and those in the free form. Part 2. *Cryst. Eng.* **2003**, *6*, 109-122.
21. Ostasz, A.; Łyszczek, R.; Mazur, L.; Tarasiuk. B. Co-crystal formation between 2-amino-4,6-dimethylpyrimidine and a new *p*-xylylene-bis(thioacetic) acid. *CrystEngComm* **2014**, *16*, 10262-10272.
22. Adsmond, D.A.; Sinha, A.S.; Khandavilli, U.B.R.; Maguire, A.R.; Lawrence, S.E. Design and synthesis of ternary cocrystals using carboxyphenols and two complementary acceptor compounds. *Cryst. Growth Des.* **2016**, *16*, 59-69.
23. Zong, Y.; Shao, H.; Pang, Y,; Wang, D.; Liu, K.; Wang, L. Multicomponent hydrogen-bonding organic solids constructed from 6-hydroxy-2-napthoic acid and N-heterocycles: Synthesis, structural characterization and synthon discussion. *J. Mol. Struct.* **2016**, *1115*, 187-198.
24. Singh, M.P.; Tarai, A.; Baruah, J.B. Neuytal, zwitterions, ionic forms of 5-aminoisophthalic acid in cocrystals, salts and their optical properties. *ChemistrySelect* **2019**, *4*, 5427-5436.
25. Thirumurugan, R.; Anitha, K. Experimental and theoretical investigations on a hydrous organic salt of 2,4,6-triaminopyrimidine-1,3-diium L-tartarate monohydrate (TTM). *J. Mol. Struct.* **2021**, *1237*, 130368.
26. Abidi, S.S.A.; Azim, Y.; Gupta, A.K.; Pradeep, C.P. Cocrystals of indole-3-acetic acid and indole-3-butyric acid: Synthesis, structural characterization and Hirshfeld surface analysis. *J. Mol. Struct.* **2018**, *1166*, 202-213.
27. Xing, P.; Li, Q.; Li, Y.; Wang, K.; Zhang, Q.; Wang, L. Organic salts formed by 2,4,6-triaminopyrimidine and selected carboxylic acids via variety of hydrogen bonds: Synthons cooperation, and crystal structures. *J. Mol. Struct.* **2017**, *1136*, 59-68.
28. Mapp, L.K.; Coles, S.J.; Aitipamula, S.; Novel solid forms of lonidamine: crystal structures and physicochemical properties. *CrystEngComm* **2017**, *19*, 2925-2935.
29. Li, Z.; Li, Y.; Du, F. Crystal structure of 2,4,6-pyrimidinetriamine-trifluoroacetate(1:1), $C_4H_8N_5^+C_2F_3O_2^-$, $C_6H_8F_3N_5O_2$. *Z. Kristallogr. NCS* **2012**, *227*, 519-520.
30. Garg, U.; Azim, Y.; Kar, A.; Pradeep, C.P.; Cocrystals/salt of 1-naphthaleneacetic acid and utilizing Hirshfeld surface calculations for acid−aminopyrimidine synthons. *CrystEngComm* **2020**, *22*, 2978-2989.

31. Pedireddi, V.R.; Chatterjee, S.; Ranganathan, A.; Rao, C.N.R.; A study of supramolecular hydrogen bonded complexes formed by aliphatic dicarboxylic acids with azaaromatic donors. *Tetrahedron*, **1998**, *54*, 9457-9474.
32. Sienkiewicz-Gromiuk, J.; Tarasiuk, B.; Mazur, L. New organic single crystal of (benzylthio)acetic acid: Synthesis, crystal structure, spectroscopic (ATR-FTIR, ^{1}H and ^{13}C NMR) and thermal characterization. *J. Mol. Struct.* **2016**, *1110*, 65-71.
33. Sienkiewicz-Gromiuk, J.; Drzewiecka-Antonik, A. The first noncovalent-bonded supramolecular frameworks of (benzylthio)acetic acid with proline compounds, isonicotinamide and tryptamine. *Molecules* **2022**, *27*, 8203.
34. *CrysAlis PRO* v. 1.171.37.35g; Agilent Technologies Ltd., Oxford, UK, 2014.
35. Sheldrick, G.M. A short history of *SHELX*. *Acta Cryst.* **2008**, *A64*, 112-122.
36. Sheldrick, G.M. Crystal structure refinement with *SHELXL*. *Acta Cryst.* **2015**, *C71*, 3-8.
37. Farrugia, L.J. *WinGX* and *ORTEP* for Windows: an update. *J. Appl. Cryst.* **2012**, *45*, 849-854.
38. Macrae, C.F.; Sovago, I.; Cottrell, S.J.; Galek, P.T.A.; McCabe, P.; Pidcock, E.; Platings, M.; Shields, G.P.; Stevens, J.S.; Towler, M.; Wood, P.A. *Mercury 4.0*: From visualization to analysis, design and prediction. *J. Appl. Crystallogr.* **2020**, *53*, 226-235.
39. Sienkiewicz-Gromiuk, J. DFT approach to (benzylthio)acetic acid: Conformational search. Molecular (monomer and dimer) structure, vibrational spectroscopy and some electronic properties. *Spectrochim. Acta A* **2018**, *189*, 116-128.
40. Prabavathi, N.; Nilufer, A.; Krishnakumar, V.; Akilandeswari, L. Spectroscopic, electronic structure and natural bond analysis of 2-aminopyrimidine and 4-aminopyrazolo[3,4-d]pyrimidine: A comparative study. *Spectrochim. Acta A* **2012**, *96*, 226-241.
41. Rospenk, M.; Koll, A. Self-assembly of 2-aminopyrimidines in nonpolar solvents. *J. Mol. Struct.* **2007**, *844-845*, 232-241.
42. Fu, W.-W.; Liu, Y.; Huang, G.; Zhu, X.-M. 4,6-dimethylpyrimidin-2-amine. *Acta Cryst.* **2013**, *E69*, o32.
43. Lin, C.-H.; Guo, H.-M.; Jian, F.-F. Crystal structure of 2-amino-4,6-dimethylpyrimidine hydrate, $(C_6H_9N_3)_{10}\cdot H_2O$. *Z. Kristallogr. NCS* **2008**, *223*, 511-512.
44. Singaravelan, K.; Chandramohan, A.; Madhankumar, S.; Enoch, M.V.; Vinitha, G. Structural characterization, computational and biological studies of a new third order NLO (1:1) organic adduct: 2-Aminopyrimidine:3-nitrophthalic acid. *J. Mol. Struct.* **2019**, *1194*, 57-65.
45. Li, Z.; Huang, J.; Meng, A.; Zheng, B. Crystal Structure, energy band and optical properties of benzoic acid—2,amino-4,6-dimethylpyrimidine (1:1) co-crystals. *J. Struct. Chem.* **2010**, *51*, 53-59.
46. Sundaraganesan, N.; Joshua, B.D.; Meganathan, C.; Sebastian, S. Vibrational spectroscopic studies supported by HF/DFT calculations of 2,4,6-triaminopyrimidine. *Indian J. Chem.* **2008**, *47A*, 821-829.